Supporting Information

Catalytically active porous coordination polymer based on a dinuclear rhodium paddle-wheel unit

Georg Nickerl,[a] Ulrich Stoeck,[a] Ulrich Burkhardt,[b] Irena Senkovska[a] and Stefan Kaskel*[a]

[a] Department of Inorganic Chemistry, Dresden University of Technology, Bergstraße 66, 01069 Dresden, Germany. Fax: +49 351 46337287; Tel: +49 351 46334885; E-mail: stefan.kaskel@chemie.tu-dresden.de
[b] Max Planck Institute for Chemical Physics of Solids, Nöthnitzer Str. 40, 01187 Dresden, Germany.

1. General information

All commercially available reagents were used without further purification. 1,3,5-Tris(4-carboxyphenyl)benzene (H_3btb) was synthesized according to a literature procedure.[1]

Powder X-ray diffraction (PXRD) patterns were collected in transmission geometry with a STOE STADI P diffractometer operated at 40 kV and 30 mA with monochromatic Cu-Kα1 (λ = 0.15405 nm) radiation and with a scan speed of 30 s/step and a step size of 0.1°.

The supercritical drying was performed in the following manner: As-made samples were washed several times with anhydrous methanol. The samples under solvent were placed in a Jumbo Critical Point Dryer 13200J AB (SPI Supplies). Methanol was exchanged several times with liquid carbon dioxide (purity: 99.995%) at 15 °C over 20 h. After that the carbon dioxide was heated up beyond the critical point and the supercritical carbon dioxide was released.

The nitrogen and hydrogen physisorption isotherms were measured on a Belsorp Max apparatus at 77 K using high purity gases (N_2 99.999%, H_2 99.999%, CO_2 99.999%). BET surface areas were determined using multipoint analysis in the relative pressure range from 0.01 to 0.1. The total pore volume was determined at $p/p_0 = 0.99$ and the micropore volume at $p/p_0 = 0.20$. Pore size distribution was obtained by applying the QS-DFT equilibrium model for nitrogen on carbon with slit pores at 77 K. The carbon monoxide sorption experiment was performed using a NOVA 2000 apparatus from Quantachrome.

Thermal analyses (TA) were carried out under air atmosphere using a Netzsch STA 409 thermal analyzer with rate of 5 K min^{-1}.

Infrared spectra (IR) were recorded in diffuse reflection geometry using a BIORAD Excalibur FTS3000 (Varian Inc.) infrared spectrometer.

The elemental analysis for C and H were performed with CHNS 932 analyzer (LECO). Samples of DUT-82 and DUT-83 were activated at 150 °C under dynamic vacuum prior to elemental analysis.

The catalytic tests were monitored by GC-MS-analysis (SHIMADZU GCMS QP5000 with a BPX5 SGE column).

Carbon monoxide breakthrough measurements were carried out using a N_2/CO gas mixture: 1 % CO in nitrogen. The flow rate was held at 42 ml/min. Experiments were carried out with 0.0255 g adsorbent at room temperature (22 °C). After the first breakthrough experiment, carbon monoxide was desorbed using helium and the second breakthrough experiment was performed on the same sample.

SEM images were done using a Zeiss DSM 982 Gemini device.

2. Synthesis

DUT-82

40.0 mg (0.09 mmol) rhodium(II) acetate and 21.0 mg (0.1 mmol) trimesic acid are filled under argon atmosphere into a pressure tube. After adding 10 ml anhydrous MeOH the pressure tube is tightly sealed and heated to 100 °C for five days. The resulting green gel-like precipitate was washed several times with dry methanol, which was afterwards exchanged with liquid carbon dioxide. The carbon dioxide was removed in a supercritical state yielding a green powder. Further activation was achieved by heating the sample at 150 °C under dynamic vacuum. Yield: 80 % based on rhodium.

DUT-83

8.0 mg (0.018 mmol) rhodium(II) acetate and 8.8 mg (0.02 mmol) 4,4′,4″-benzene-1,3,5-triyl-tris(benzoic acid) are filled under argon atmosphere into a pressure tube. After adding 10 ml anhydrous MeOH the pressure tube is tightly sealed and heated to 100 °C for five days. The resulting green gel-like precipitate was washed several times with dry methanol, which was afterwards exchanged with liquid carbon dioxide. The carbon dioxide was removed in a supercritical state yielding a green powder. Further activation was achieved by heating the sample at 150 °C under dynamic vacuum. Yield: 65 % based on rhodium.

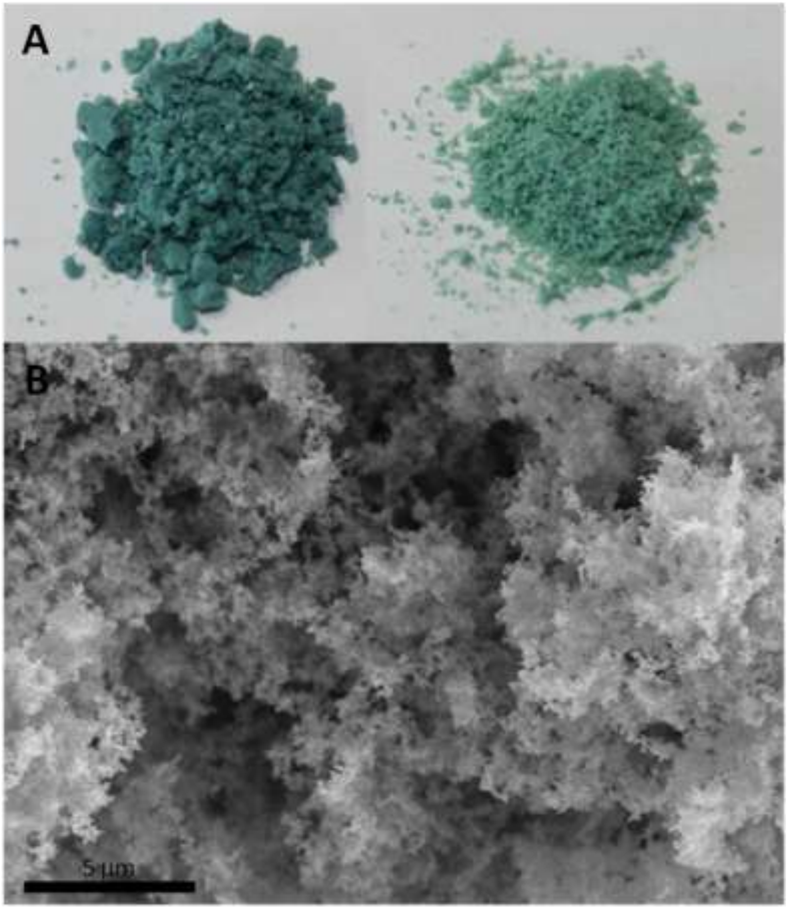

Figure S1: Supercritically dried DUT-82 (A left) and additional termally activated DUT-82 (A right). SEM image of DUT-82 (B) shows a typical aerogel structure.

3. XRD data

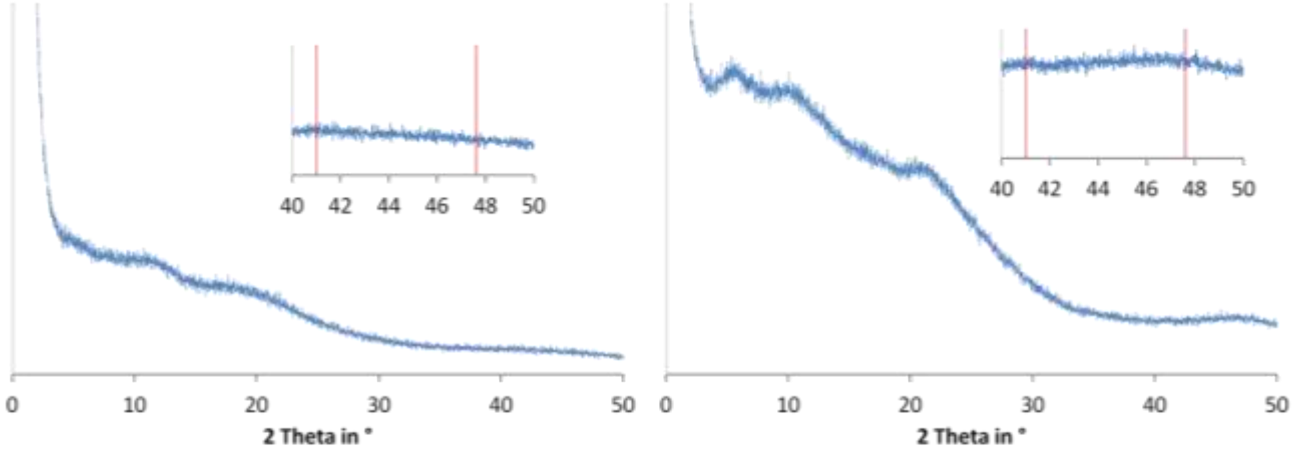

Figure S2: PXRD pattern of DUT-82 (left) and DUT-83 (right). Red vertical lines indicate the theoretical position of diffraction peaks corresponding to elemental rhodium.

The XRD patterns show the lack of long range order in DUT-82 and DUT-83. It also proves that there are no rhodium black impurities after synthesis.

4. XAS data

The local environment of the Rh atoms was investigated on basis of the X-ray absorption spectra at the Rh K-edge (23220 eV). The spectra in the energy range 22870 eV < E < 24420 eV were recorded at beamline C of Hasylab at DESY using the Si(311) double crystal monochromator.[2] A constant step width of $\Delta k = 0.05$ Å^{-1} was used. The absorption coefficients $\mu_{sample}(E) = -\ln(C2/C1)$ of the "SAMPLE" and the reference (5 layers of 0.1 µm Rh foil (99.9 Goodfellow)) $\mu_{ref}(E) = -\ln(C3/C2)$ was calculated from the intensities C1, C2 and C3 detected by ionisation chambers in front and behind the transmitted sample and reference materials. Approx. 20 mg of the nanopowder samples were wrapped in Kapton® foil on the beamline sample holders.

Data processing, analyses and fitting have been performed with the horae software package.[3] The background removal according to the spline fitting of the autobk modul revealed a step height of 0.32. µ(E) was obtained after normalisation and background subtraction (Figure S3). Significant EXAFS modulation are found up to k = 15 Å^{-1} (Figure S4). The Fourier transformation in the k-range 2 Å^{-1} < k < 15 Å^{-1} was performed with the hanning window-type and resulted the radial distribution function $\chi(R)$ presented in Figure S4.

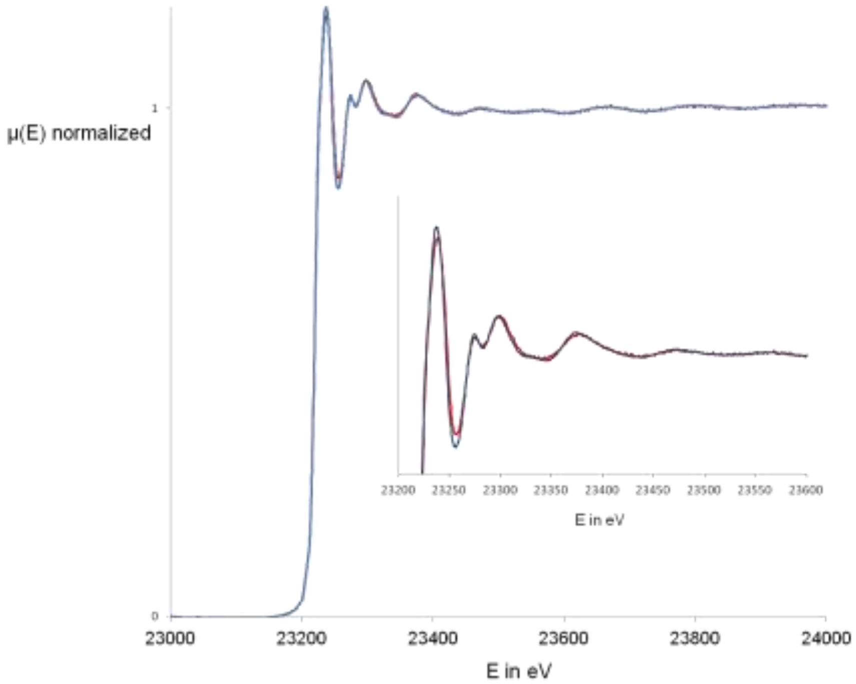

Figure S3: μ(E) of DUT-83 (red) and $Rh_2(OAc)_4 \cdot 2$ MeOH (blue).

The agreement between rhodium(II) acetate and supercritically dried but not thermally activated DUT-82 shows that DUT-82 consists of dinuclear rhodium paddle-wheel units. Furthermore the paddle-wheel is coordinated by methanol in axial positions after supercritical drying.

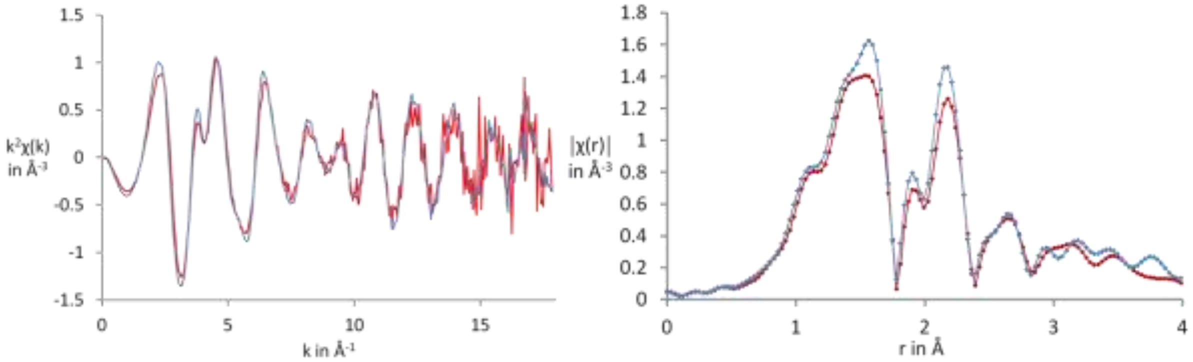

Figure S4: X-ray absorption fine structure (left) of DUT-82 (red) and $Rh_2(OAc)_4 \cdot 2$ MeOH (blue) and their fourier transformed representation in R-space (right).

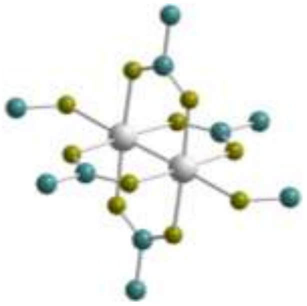

Figure S5: Structure of $Rh_2(OAc)_4 \cdot 2MeOH$ derived from single crystal structure analysis (rhodium grey, carbon blue, oxygen green, hydrogen atoms omitted).

To further investigate the XAS data, the measured data was compared with data calculated from the known structure of rhodium(II) acetate in the solid state (Figure S5) derived from single crystal structure determination.[4] Figure S6 shows the data for DUT-82, rhodium(II) acetate and the curve for the scattering path resulting from a rhodium atom surrounding the central atom. It can be seen that the interatomic distance is represented correctly.

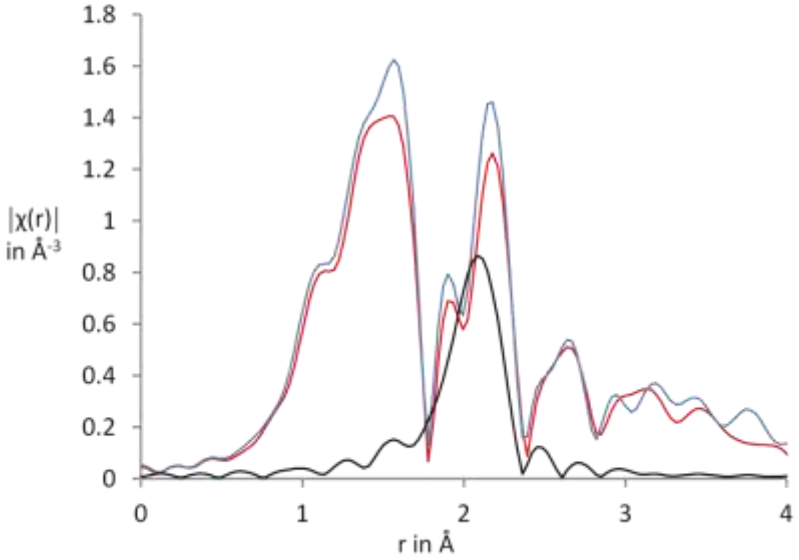

Figure S6: Radial distribution of atoms around Rh in DUT-82 (red), $Rh_2(OAc)_4 \cdot 2\ MeOH$ (blue). The black curve indicates the calculated path derived from the Rh-atom surrounding the central atom.

5. Thermogravimetric analysis

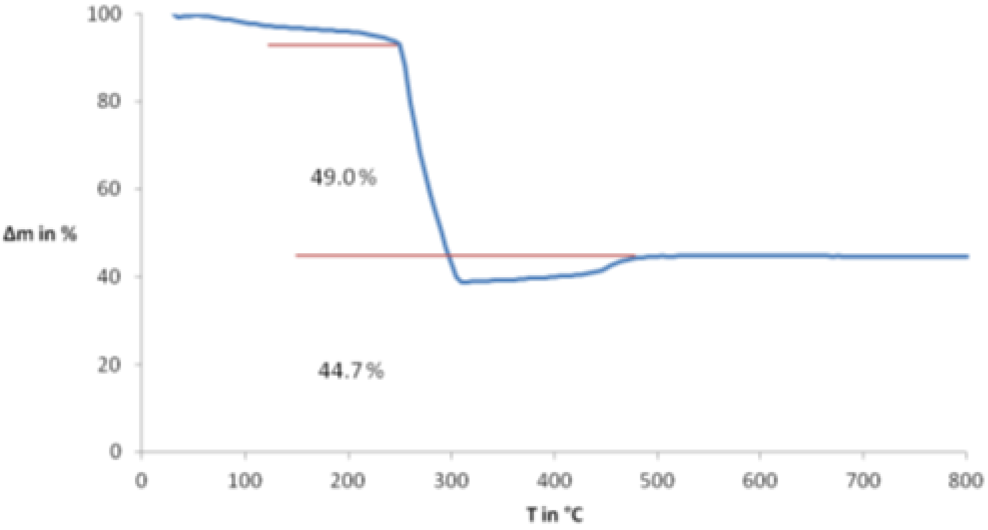

Figure S7: Thermogravimetric analysis data of DUT-82.

The TG of supercritically dried and thermally activated DUT-82 reveals thermal stability up to 250 °C. The mass rise between 300 °C to 500 °C is due to the complete oxidation to rhodium(III) oxide, which was proven by XRD. From the residual mass a rhodium content of around 36 % can be calculated.

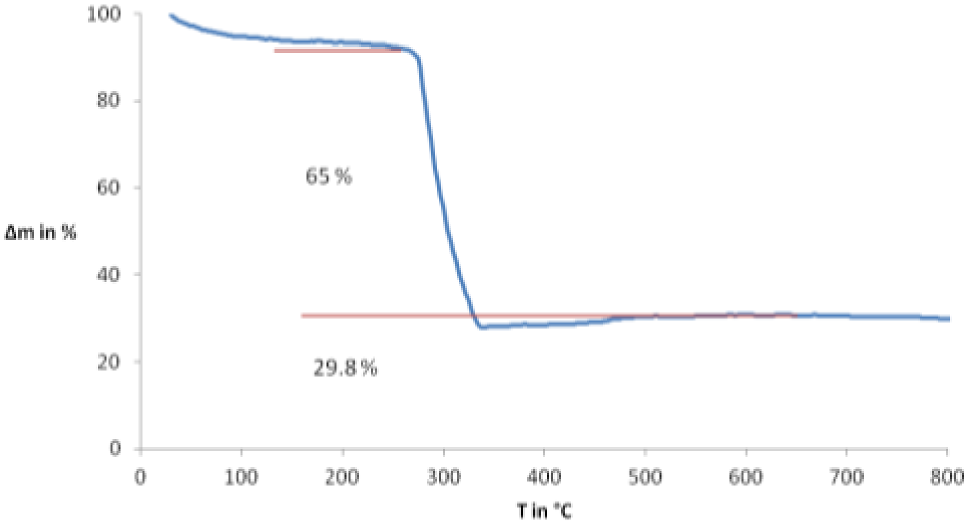

Figure S8: Thermogravimetric analysis data of DUT-83.

The TG of supercritically dried and thermally activated DUT-83 reveals thermal stability up to 250 °C. As for DUT-82, the mass rise between 300 °C to 500 °C is due to the complete oxidation to rhodium(III) oxide, which was proven by XRD. From the residual mass a rhodium content of around 24 % can be calculated.

6. Elemental analysis

Table S1: Comparison of elemental analysis for DUT-82 with calculated values.

element	$Rh_2(OAc)_4$	DUT-82	$Rh_3(btc)_2$ (theo.)
carbon in %	21.7	25.6	29.9
hydrogen in %	2.7	2.3	0.8
rhodium in %	46.6	ca. 36*	42.7

* calculated from thermal gravimetric analysis

Elemental analysis for DUT -82 indicates that the exchange reaction between acetate and trimesate is not complete and thus the rhodium paddle-wheel unit is coordinated by trimesate- as well as acetate-ligands. Probably not every carboxylic group of the trimesic acid is deprotonated leading to the low rhodium content (and to the relatively high hydrogen content). Furthermore, it should be noted, that slight variations in composition are probable for each batch.

Table S2: Comparison of elemental analysis for DUT-82 with calculated values.

element	$Rh_2(OAc)_4$	DUT-83	$Rh_3(btb)_2$ (theo.)
carbon in %	21.7	46.0	55.0
hydrogen in %	2.7	2.5	2.6
rhodium in %	46.6	ca. 24*	26.2

* calculated from thermal gravimetric analysis

As for DUT-82, the elemental analysis for DUT-83 indicates a presence of btb- and acetate-ligands in the structure of DUT-83.

7. IR data of DUT-83

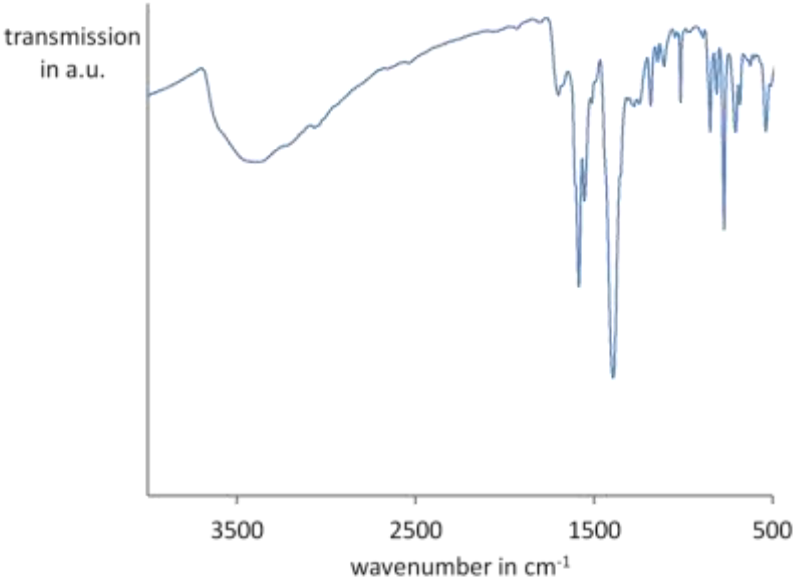

Figure S9: IR data of DUT-83.

8. Nitrogen physisorption data

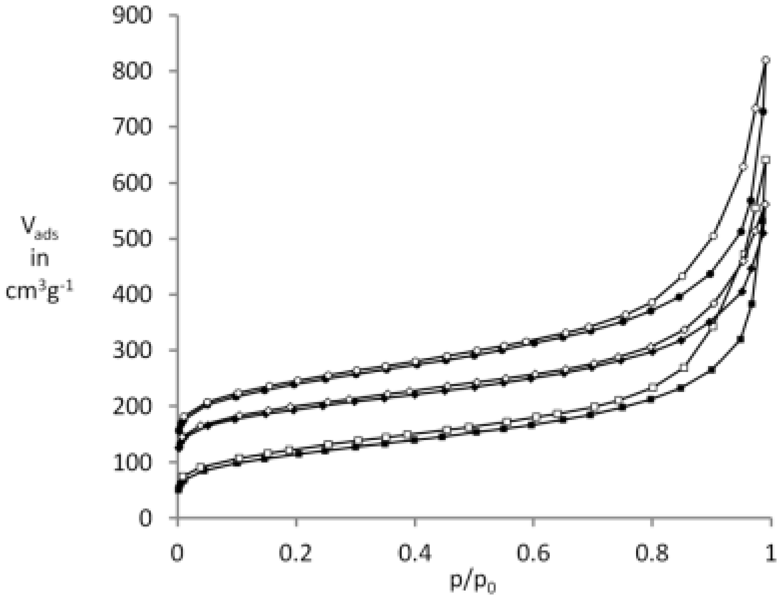

Figure S10: Nitrogen isotherms of DUT-82 after supercritical drying (squares), after supercritical drying and additional activation at 100 °C (diamonds), after supercritical drying and additional activation at 150 °C (circles). Solid symbols illustrate the adsorption branches and open symbols the desorption branches.

9. Pore size distribution of DUT-82

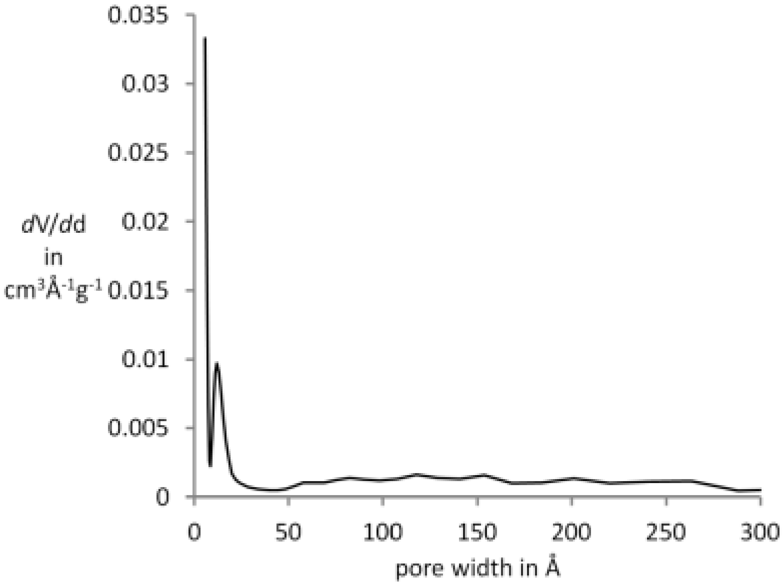

Figure S11: Pore size distribution of DUT-82.

The pore size distribution of DUT-82 reveals a maximum at 12 Å which is close to the size of the largest pores of HKUST-1 being 9 Å in diameter.

10. Hydrogen physisorption data

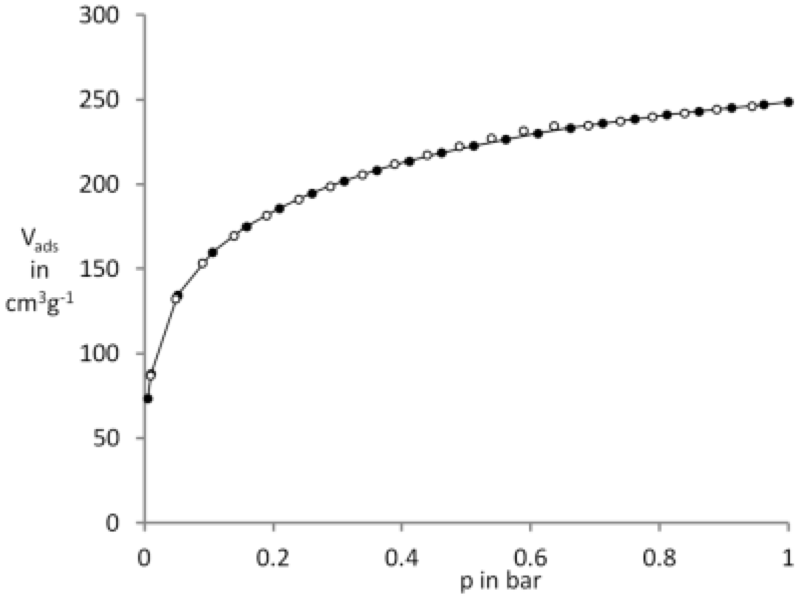

Figure S12: Hydrogen physisorption isotherm of DUT-82 at 77 K. Solid symbols illustrate the adsorption branche and open symbols the desorption branche.

11. Carbon dioxide physisorption data

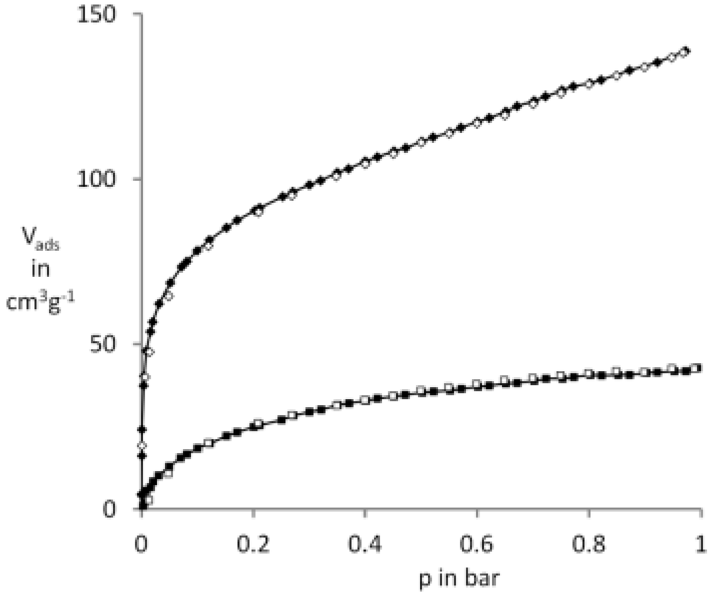

Figure S13: Carbon dioxide physisorption isotherms of DUT-82 at 273 K (squares) and 196 K (diamonds). Solid symbols illustrate the adsorption branches and open symbols the desorption branches.

12. Carbon monoxide breakthrough measurements and adsorption data

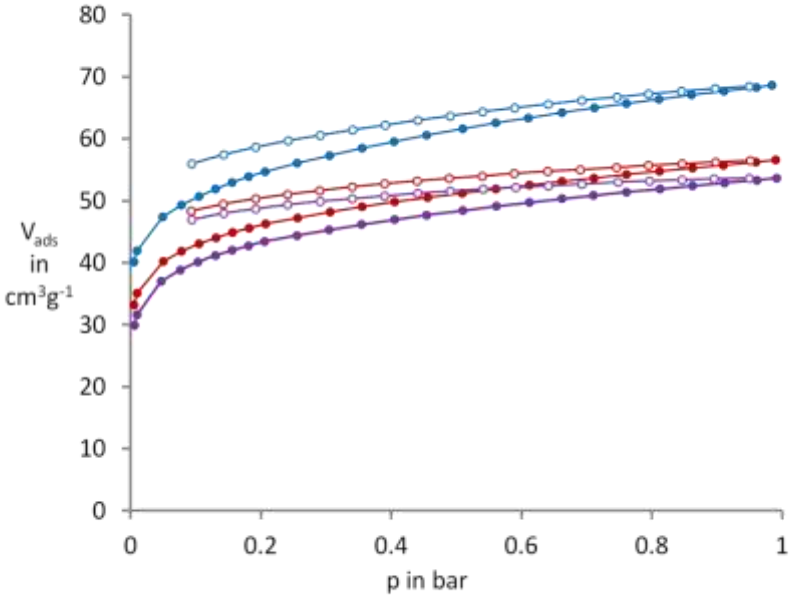

Figure S14: Carbon monoxide adsorption isotherms of DUT-82 at 298 K (blue), 273 K (red) and 258 K (purple). Solid symbols illustrate the adsorption branches and open symbols the desorption branches.

Figure S15: DUT-82 colour turns form pale green to dark green/grey upon carbon monoxide adsorption.

DUT-82 changes colour upon carbon monoxide adsorption. However, the change in color is reversible if DUT-82 is activated at 150 °C under dynamic vacuum.

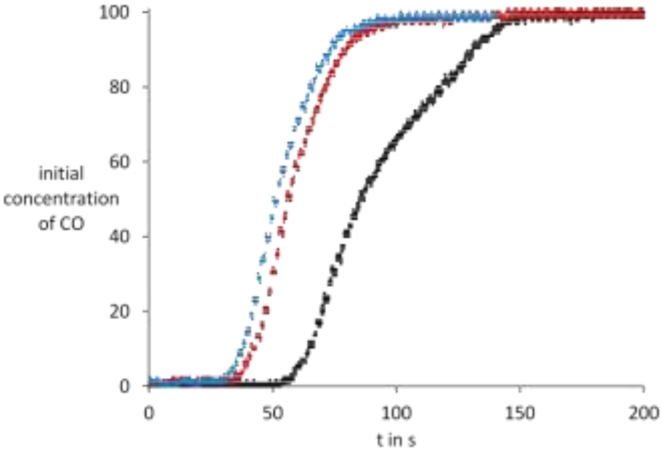

Figure S16: Carbon monoxide breakthrough curves of DUT-82 (1st cycle, black; 2nd cycle, red; 3rd cycle, blue).

The loss of capacity of DUT-82 for carbon monoxide after the first cycle to a constant capacity proves that carbon monoxide is not fully removed from DUT-82 by flushing with helium after the first cycle.

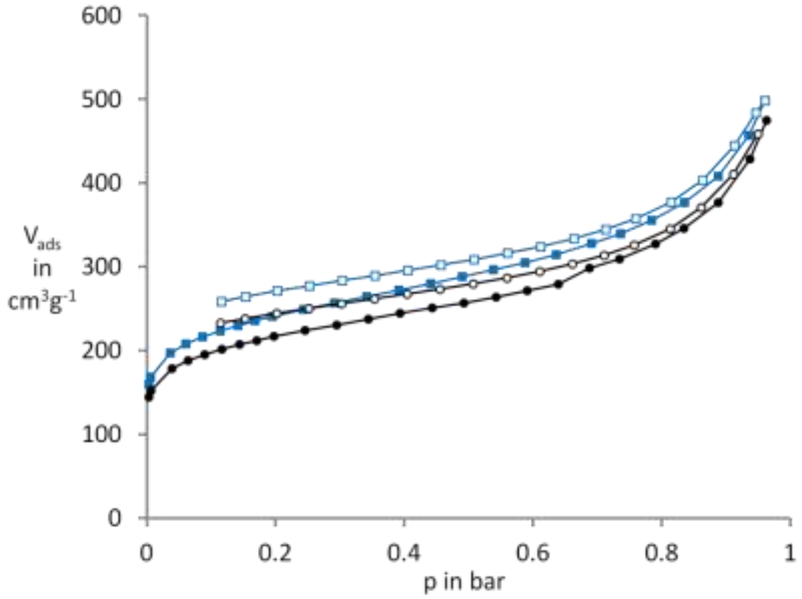

Figure S17: Carbon monoxide adsorption isotherms of DUT-82 at 77 K. 1st cycle blue, 2nd cycle black.

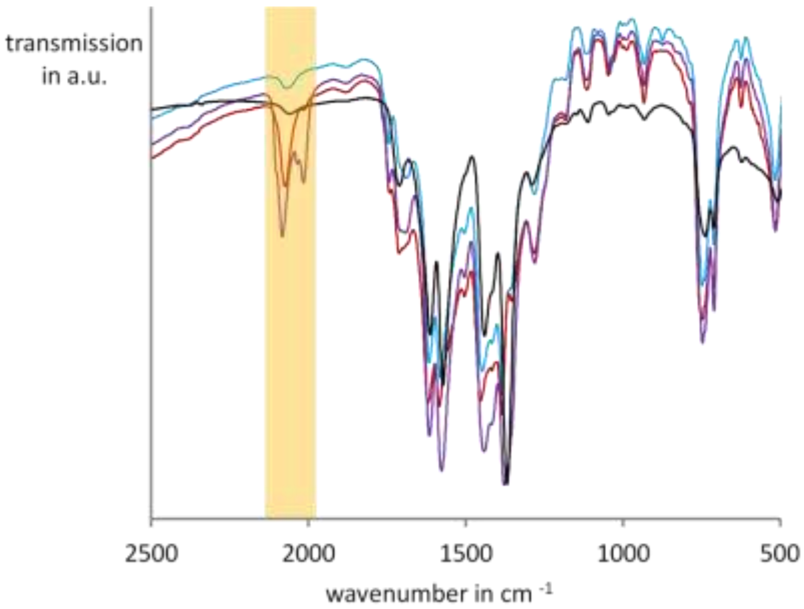

Figure S18: IR spectra of DUT-82 (light blue), DUT-82 after adsorption of carbon monoxide (red), after carbon monoxide adsorption followed by activation at room temperature (purple), after carbon monoxide adsorption followed by activation at 150 °C (black).

The band at 2080 cm^{-1} in the IR spectra indicates bonded carbon monoxide compared to carbon monoxide in the gas phase showing a band at 2143 cm^{-1}. In addition, the spectra show that carbon monoxide cannot be completely removed from DUT-82 by simply applying vaccum, but needs additional heating. This finding is furthermore supported by the carbon monoxide adsorption isotherm, in which the desorption branch do not match the adsorption branch.

13. Catalysis data

For catalytic investigations 9.7 mg DUT-82 were charged into a Schlenk tube and activated at 150 °C under dynamic vacuum overnight. After cooling down to 40 °C the tube was charged with hydrogen (p = 1 bar). After 30 min 100 mg styrene in 5 ml *n*-heptane were added defining the starting point of the catalysis. Henceforward consecutive samples of 0.1 ml were taken via a syringe with a syringe filter (pore width 200 nm) and diluted with 0.5 ml of *n*-heptane. The samples were investigated by GC-MS. The ratio between ethylbenzene and styrene was determined by comparison of the peak areas.

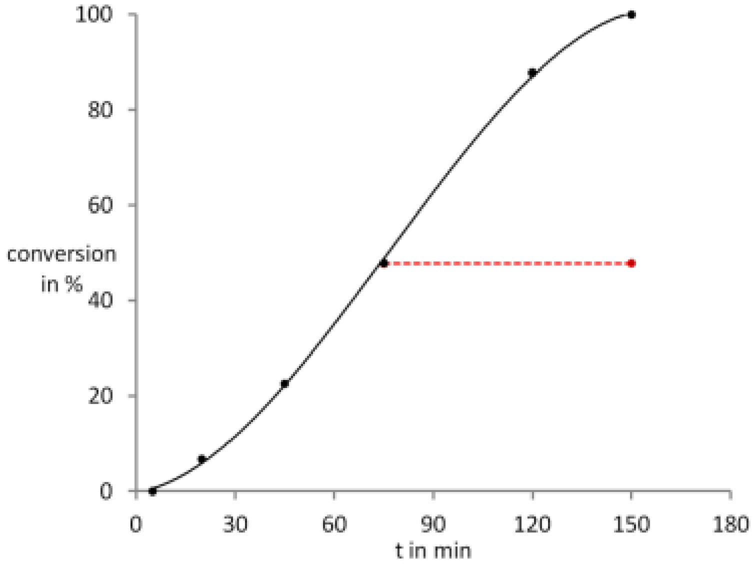

Figure S19: Time course of the hydrogenation of styrene catalysed by DUT-82 (black circles) and the test of heterogeneity after removing a sample after 90 min (red circle).

Kinetic investigations reveal an induction period after which the conversion increases in a linear manner over time. An induction period was already observed by Mori et al. for the hydrogenation of propene and 1-butene catalysed by rhodium(II) carboxylate polymer complexes. Mori et al. concluded that the induction period in their experiments is due to the adsorption of the product within the porous material.[5]

After 90 min and around 50 % conversion 0.5 ml of sample for the heterogeneity test was taken *via* a syringe with a syringe filter (pore width 200 nm) and subject to identical conditions as the reaction catalysed by DUT-82. The sample for the heterogeneity test was a colorless liquid. After 180 min when the reaction catalysed by DUT-82 reached 100 % conversion, the sample for the heterogeneity test was also investigated concerning the ratio of ethylbenzene and styrene. As the ratio stayed constant the true heterogeneous character of DUT-82 was proven.

The turn over number (TON) is 29 per cycle amounting to 290 after ten cycles. The corresponding turn over frequency is 11.6 h^{-1}. These results are in the range for other MOF catalysts. E.g., the hydrogenation of 1-octene with $[Pd(2\text{-pymo})_2]_n$ 3 H_2O as catalyst shows a TON of 25 along with a degradation of the catalyst (see ref. 21). However, silica supported rhodium catalysts show TONs much higher than DUT-82 (see ref. 45). In contrast, rhodium acetate achieves only a conversion of 17 % after 24 h under identical conditions. This might be due to the partial insolubility of rhodium(II) acetate in *n*-heptane.

To investigate whether the porosity of DUT-82 changes during the course of reaction a sample of DUT-82 was subject to a supercritical drying after ten catalytic cycles. After exchanging ethylbenzene and *n*-heptane from the catalysis against methanol the sample was dried using supercritical carbon dioxide in the same way as initially DUT-82. Although uptake of nitrogen in the lower pressure range decreased, the shape of the isotherm as well as the final uptake proof that DUT-82 preserves its porous character after ten catalytic cycles (Figure S20).

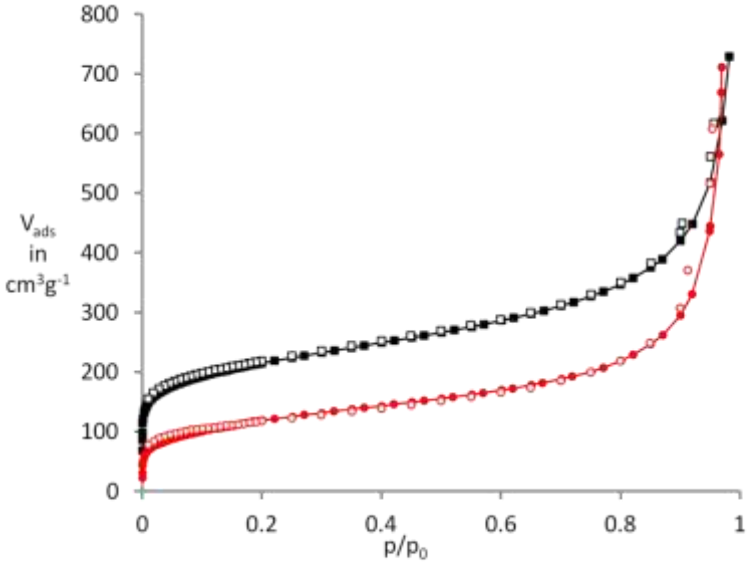

Figure S20: Nitrogen physisorption isotherms of DUT-82 (black) and DUT-82 after ten catalytic cycles (red). Solid symbols illustrate the adsorption branches and open symbols the desorption branches.

Although the appearance of DUT-82 did not change during the course of reaction, meaning that its green colour was preserved, XRD investigations after catalysis were performed to rule out the possibility of rhodium black formation during the catalysis (Figure S21).

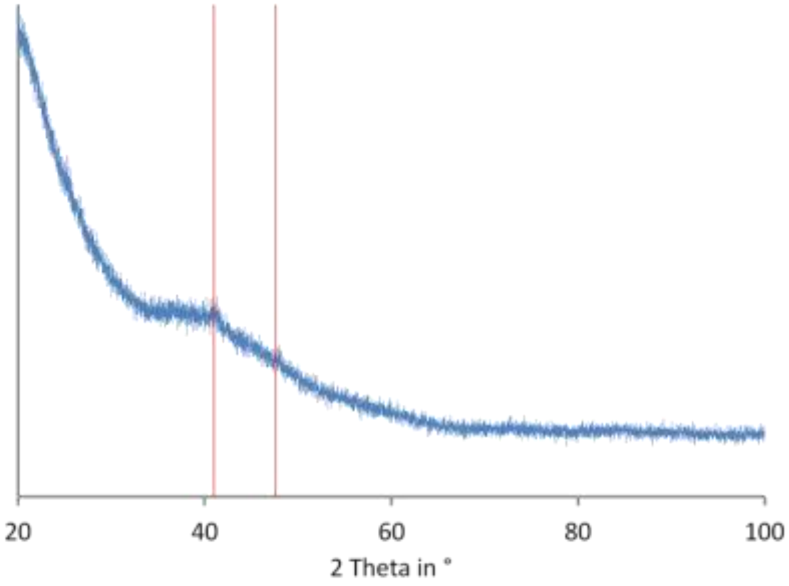

Figure S21: XRD measurements of DUT-82 after ten catalytic cycles up to 100 % conversion.

14. References

1 J. Palomero, J. A. Mata, F. Gonzalez, E. Peris, *New J. Chem.* 2002, **26**, 291; M. V. Vasylyev, R. Neumann, *J. Am. Chem. Soc.*, 2004, **126**, 884.

2 K. Rickers, W. Drube, H. Schulte-Schrepping, E. Welter, U. Brüggmann, M. Herrmann, J. Heuer, H. Schulz-Ritter, *AIP Conference Proceedings*, 2007, 882(X-Ray Absorption Fine Structure (XAFS13)), 905; K. Rickers, U. Brüggmann, W. Drube, M. Herrmann, J. Heuer, E. Welter, H. Schulte-Schrepping, H. Schulz-Ritter, *AIP Conference Proceedings*, 2007, 879 (Pt. 1, Synchrotron Radiation Instrumentation, Part 1), 907.

3 M. Newville, *J. Synchrotron Rad.*, 2001, **8**, 322; B. Ravel, M. Newville, *J. Synchrotron Rad.*, 2005, **12**,537.

4 V. Noinville, B. Viossat, N.-H. Dung, *Acta Cryst.*, 1993, **C49**, 1297.

5 T. Sato, W. Mori, C. N. Kato, E. Yanaoka, T. Kuribayashi, R. Ohtera, Y. Shiraishi, *J. Cat.*, 2005, **232**, 186.